Does Hexagonal Lattice Improve the Performance of QAM-FBMC?

Iandra Galdino, Rostom Zakaria, Didier Le Ruyet and Marcello L. R. de Campos

Abstract—Quadrature amplitude modulation filter-bank multi-carrier (QAM-FBMC) is a promising technology for future wireless communications systems. However, the intrinsic interference observed at the receiver can be a source of problems. In order to overcome the intrinsic interference, in this paper, we propose a QAM-FBMC system with hexagonal lattice structure, which we call HQAM-FBMC. We also propose a new prototype filter design, specifically for the HQAM-FBMC system, based on discrete prolate spheroidal sequences (DPSS). The proposed filters have also been optimized to reduce the intrinsic interference of the system. Moreover, we compare and analyze the performance of the QAM-FBMC system with the performance of the proposed HQAM-FBMC using the optimized filter through the bit error rate (BER).

Index Terms—Filter-bank multicarrier, QAM-FBMC, 5G, hexagonal lattice, wireless communication.

I. INTRODUCTION

Several waveforms have been proposed and studied for the next generation of communication systems *e.g.* the fifth generation (5G) and beyond 5G (B5G) [1] [2]. Among the most prominent multicarrier proposals, we can cite the offset-quadrature amplitude modulation filter-bank multicarrier (OQAM-FBMC) [3] [4] and the quadrature amplitude modulation filter-bank multicarrier (QAM-FBMC) [5], [6]. One of its major characteristics is the per-subcarrier filtering, which allied to the usage of well-localized prototype filters can bring significant improvements when compared to the Orthogonal Frequency Division Multiplexing (OFDM). In QAM-FBMC systems, there is no need to satisfy the orthogonality condition to recover transmitted data, as required in OFDM. Hence, we can have more flexibility in the prototype filter design since the orthogonality constraint is relaxed.

In multicarrier systems, the symbol duration and subcarrier spacing define the time-frequency lattice structure associated with the communication system [7]. Most of the work on multicarrier systems design has dealt with rectangular lattices. However, such an approach does not show to be the best one for OFDM over time-frequency dispersive channels as discussed in [8].In those dispersive channels, the transmitted signal is spread in time and in frequency, causing intersymbol interference (ISI) and interchannel interference (ICI). With the aim of reducing as much as possible the interference of

Iandra Galdino is with Department of Computer Science, Fluminense Federal University (UFF), Niterói 24210-240, Brazil, e-mail iandra.galdino@smt.ufrj.br

Marcello L. R. de Campos is with Electrical Engineering Program, Federal University of Rio de Janeiro (UFRJ) Rio de Janeiro, Brazil

Rostom Zakaria and Didier Le Ruyet are with the CEDRIC/LAETITIA Laboratory, CNAM, Paris 75141, France

the OFDM transmitted signal, the authors in [8] proposed to use basic signals which are localized in time and frequency with the same time frequency scale as the channel itself. It means to choose the prototype filter parameters and the lattice parameters such that they adapt the signal to the channel characteristics [9], [10]. Their prototype filter approach has already been introduced to some extent in [10]–[12]. They have introduced the lattice OFDM (LOFDM) systems, which are based on general, non-rectangular, time-frequency lattices. They have also demonstrated that the LOFDM outperforms the classical OFDM.

Several lattice structures, including hexagonal (or quincunx) structures, have been widely studied in [13]. More recently, in [14]–[16], the hexagonal lattice structure was studied in multicarrier faster than Nyquist systems (MFTN), and also in OFDM. As in [8], the authors evaluated the systems performance when using Gaussian filter. To the best of our knowledge, there is no work in the literature addressing the hexagonal lattice applied to QAM-FBMC systems. Hence, we propose in this paper a hexagonal structure of conventional QAM-FBMC, which we call HQAM-FBMC. Different prototype filters have been proposed in the literature [6] [17] [18]. A novel prototype filter design and optimization for standard QAM-FBMC systems have been developed in [19]. The authors proposed a filter based on discrete prolate spheroidal sequences (DPSS), and then optimized the proposed filter to overcome the intrinsic interference of the system. On the basis of their approach, we propose in this paper a prototype filter design for multicarrier systems with hexagonal lattice structure, also based on the DPSS. Then, we optimize the proposed filter to reduce the intrinsic interference of the HQAM-FBMC system.

Furthermore, we also provide a performance comparison of the QAM-FBMC system using the DPSSb filter proposed in [19], and the proposed HQAM-FBMC system with our proposed and optimized HDPSSb prototype filter. Finally, we compare and discuss the advantages of using a rectangular and hexagonal lattice in the QAM-FBMC system when applying appropriately optimized prototype filters. The main contributions of this paper can be summarized as follows:

- Design optimized prototype filters for hexagonal QAM-FBMC.
- Perform a fair performance comparison of rectangular QAM-FBMC and hexagonal QAM-FBMC considering AWGN and pedestrian channels.
- Show that HQAM-FBMC outperforms QAM-FBMC with optimized filters considering 4-QAM modulation and pedestrian channels.

- Show that while a gain can be obtained with hexagonal compared to rectangular QAM-FBMC when using Gaussian filters, this conclusion cannot be generalized to all classes of optimized filters when using high-efficiency modulations.

For the sake of clarity, we start by presenting in Section II the QAM-FBMC system model with conventional rectangular lattice and hexagonal lattice. In Section III we present our prototype filter proposal based on DPSS. The optimization results are presented in Section IV. We evaluate the system performance through simulations in Section V. Finally, the conclusions are drawn in Section VI.

II. SYSTEM MODEL

In this section we present the system model for the standard QAM-FBMC, with a rectangular lattice illustrated in Fig. 1 (a). We also present the proposed system model for QAM-FBMC with hexagonal lattice, as shown in Fig. 1 (b), which we call HQAM-FBMC.
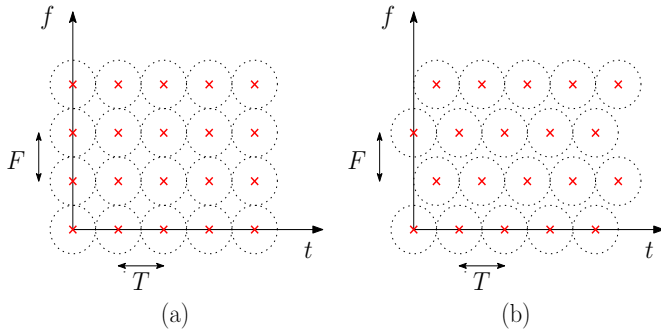

Fig. 1: Time-frequency lattice structure, (a) rectangular and (b) hexagonal.

A lattice corresponds to a set of algebraic coordinates of the filters in the time-frequency plane [7], [8], [13], [14]. In practice, it is a set generated by sampling the time-frequency plane in the red markers as exemplified in Fig. 1. A lattice Λ can be described by its non-unique generator matrix $\boldsymbol{L}$. The generator matrix contains the coordinates of the column vectors that describe the fundamental domain of a lattice [8].

The lattice geometry is defined by its generator matrix. For example, the generator matrix

$$\boldsymbol{L}_R = \begin{bmatrix} T & 0 \\ 0 & F \end{bmatrix} \qquad (1)$$

yields a rectangular lattice Λ_R presented as exemplified in Fig. 1 (a), with a symbol duration T and frequency spacing F. Similarly, a hexagonal lattice [7], [8], [13], [14] Λ_H can be obtained from a generator matrix

$$\boldsymbol{L}_H = \begin{bmatrix} T & 0.5T \\ 0 & F \end{bmatrix} \qquad (2)$$

as exemplified in Fig. 1 (b).

A. Rectangular QAM-FBMC

Let us consider a baseband QAM-FBMC signaling system with M subchannels. By defining $d_{k',n'}$ as the transmitted

symbol allocated at the k'-th subcarrier and transmitted in the n'-th QAM-FBMC symbol, the QAM-FBMC standard transmitted signal, can be given by

$$s(t) = \sum_{n'} \sum_{k'=0}^{M-1} d_{k',n'} g(t - n'T) e^{j2\pi Fk't}, \qquad (3)$$

where $g(t)$ is assumed to be an unit-energy prototype filter i.e., $\int_{-\infty}^{\infty} |g(t)|^2 dt = 1$, with overlapping factor K, and length $L_g = KM$. The symbol time is represented by T, and F is the subcarrier spacing.

In order to derive the expression of the intrinsic interference, we consider an Additive White Gaussian Noise (AWGN) channel for the sake of simplicity. In that case, the continuous-time received signal can be described as

$$r(t) = s(t) + v(t), \qquad (4)$$

where $v(t)$ is Gaussian white noise.

After a filter that matches the transmission time-frequency shift, the output of the k-th matched filter at a time instant n is given by [19]

$$\tilde{d}_{k,n} = d_{k,n} + \underbrace{\sum_{(k',n') \neq (k,n)} d_{k',n'} A_g(\Delta_n T, \Delta_k F)}_{\text{interference}} + v_{k,n} \qquad (5)$$

where $A_g(\tau, \nu)$ is the ambiguity function [20], the Gaussian noise at the k-th subcarrier at a time instant n is defined by $v_{k,n} = \int_{-\infty}^{\infty} v(t) g^*(t - nT) e^{-j2\pi Fkt} dt$, $\Delta_n = n - n'$, and $\Delta_k = k - k'$.

The total interference over the k-th subcarrier at the n-th time instant, which comes from the surrounding symbols (k', n') can be calculated by

$$I_{k,n} = \sum_{(k',n') \in \Upsilon_{k,n}} d_{k',n'} \Gamma_{\Delta_k, \Delta_n}, \qquad (6)$$

where $\Gamma_{\Delta_n, \Delta_k} = A_g(\Delta_n T, \Delta_k F)$ are the intrinsic interference coefficients and $\Upsilon_{k,n}$ is the set of (k', n') for which the interference coefficient is non-null.

B. Hexagonal QAM-FBMC

Let us consider a baseband HQAM-FBMC signaling system with M subchannels. Also, considering $d_{k',n'}$ as the transmitted symbol allocated at the k'-th subcarrier and transmitted in the n'-th QAM-FBMC symbol, the transmitted HQAM-FBMC signal can be expressed as [15]

$$s(t) =$$
$$\sum_{n'} \sum_{k'=0}^{M-1} d_{k',n'} g\left(t - n'T - \frac{\text{mod}(k', 2)}{2}T\right) e^{j2\pi Fk't} \qquad (7)$$

where mod(.) represents the modulo operation.

Similarly to the case of rectangular lattice, considering the transmission over AWGN channel at the receiver, the demodulated symbol at the k-th subcarrier and n-th symbol is given by (8), presented in the top of the next page, where $v_{k,n}$ is defined by

$$\int_{-\infty}^{\infty} v(t) g^*\left(t - nT - \frac{\text{mod}(k, 2)}{2}T\right) e^{-j2\pi Fkt} dt. \qquad (9)$$

JOURNAL OF COMMUNICATION AND INFORMATION SYSTEMS, VOL. 38, NO.1, 2023.

70

$$\tilde{d}_{k,n} = \int_{-\infty}^{\infty} r(t)g^*(t - nT - \frac{\text{mod}(k,2)}{2}T)e^{-j2\pi Fkt}dt$$

$$= \int_{-\infty}^{\infty} \sum_{n'} \sum_{k'=0}^{M-1} d_{k',n'}g\left(t - n'T - \frac{\text{mod}(k',2)}{2}T\right) g^*\left(t - nT - \frac{\text{mod}(k,2)}{2}T\right) e^{-j2\pi F(k-k')t}dt + v_{k,n}$$

$$(8)$$

Also, by setting $\Delta'_n = (n + \text{mod}(k,2)/2) - (n' + \text{mod}(k',2)/2)$, we can derive the ambiguity function as presented in (10).

Thus, we can use (10) to rewrite the demodulated symbol as

$$\tilde{d}_{k,n} = d_{k,n} + v_{k,n}$$
$$+ \underbrace{\sum_{(k',n')\neq(k,n)} d_{k',n'} A_g\left(\Delta'_n T, \Delta_k F\right) e^{-j2\pi\Delta_k\Delta'_n}}_{\text{interference}} .$$

$$(11)$$

By defining the intrinsic interference coefficients as $\Gamma_{\Delta'_n,\Delta_k} = A_g\left(\Delta'_n T, \Delta_k F\right) e^{-j2\pi\Delta_k\Delta'_n}$, the total interference observed at the receiver of a HQAM-FBMC system over the k-th subcarrier at the n-th time instant can be obtained by weighting the neighbor symbols with these coefficients as follows:

$$I'_{k,n} = \sum_{(k',n')\in\Upsilon_{k,n}} d_{k',n'}\Gamma_{\Delta'_n,\Delta_k}. \qquad (12)$$

As we can see, similar to the rectangular case, these coefficients are essential to calculate the intrinsic interference, since the quantity of $\Gamma_{\Delta'_n,\Delta_k}$, when $(k',n') \neq (k,n)$, is dedicated to the interference that comes from the surrounding symbols.

III. HEXAGONAL DPSS BASED PROTOTYPE FILTER -HDPSSB

In this section, we present a prototype filter design technique based on DPSS, specifically for the HQAM-FBMC. For this, we consider the spectral confinement, by selecting the most energy concentrate sequences among the DPSS, and minimize the intrinsic interference coefficients of the HQAM-FBMC system by using its ambiguity function.

Slepian [21] defined the discrete Prolate Spheroidal Sequences (DPSS), here called $\phi_c^{(p)}(L,B)$, as the real solution to the system of equations

$$\sum_{l=0}^{L-1} \frac{\sin\left(\pi(c-l)B\right)}{\pi(c-l)}\phi_l^{(p)}(L,B) = \lambda_p(L,B)\phi_c^{(p)}(L,B) \quad (13)$$

for $c \in \mathbb{Z}$, and $\lambda_p(L,B)$ being the eigenvalues of the sinc function kernel with length L and bandwidth B [21].

We can rewrite (13) in a matrix approach as

$$\mathbf{Q}(L,B)\boldsymbol{\phi}^{(p)}(L,B) = \lambda(L,B)\boldsymbol{\phi}^{(p)}(L,B). \qquad (14)$$

These sequences are thus seen to be the eigenvectors of the $L \times L$ matrix $\mathbf{Q}(L,B)$ with elements [21], [22]

$$\mathbf{Q}(L,B)_{l,c} = \frac{\sin(\pi(l-c)B)}{\pi(l-c)},$$
$$l,c = 0,1,2,\ldots,L-1 \qquad (15)$$

We have used here the same approach as in [19] to design and optimize the prototype filter. We start by designing a function that represents the desired prototype filter using the DPSS. We design the matrix $\mathbf{Q}(L,B)$ as presented in (15), and select the eigenvectors $\boldsymbol{\phi}^{(p)}(L,B)$ whose eigenvalues $\lambda_p(L,B)$ are higher than a certain threshold ξ. Then, we define the desired filter as

$$\boldsymbol{g} = \sum_{p=0}^{N_e-1} w_p\boldsymbol{\phi}^{(p)}(L,B). \qquad (16)$$

where $\boldsymbol{g} = [g[0],g[1],\ldots,g[L_g-1]]$ is the discrete response of $g(t)$ with $g[m] = g\left(m\frac{T}{M}\right)$, and w_p is the weight coefficient.

Taking into account the intrinsic interference of HQAM-FBMC systems described in (12), and the definition of the desired filter, we propose an optimization problem to find the best prototype filter for HQAM-FBMC systems. In this sense, we want to find the optimal weights w_p of the prototype filter that minimize the energy of the interference coefficients $\Gamma_{\Delta'_n\Delta_k}$ subject to the filter energy constraint. We formulate our optimization problem as

$$\min_{\boldsymbol{\omega}} \sum_{\substack{(k',n') \\ \neq \\ (k,n)}} \left| \sum_m g\left[m - n'M - \frac{\text{mod}(k',2)}{2}M\right] \right.$$
$$\left. \times g^*\left[m - nM - \frac{\text{mod}(k,2)}{2}M\right] e^{-j2\pi\Delta_k\frac{1}{M}m} \right|^2$$
$$\text{s.t.} \quad \boldsymbol{g}^{\text{H}}\boldsymbol{g} = 1 \qquad (17)$$

where the cost function is the discrete version of the ambiguity function given in (10).

We have solved the above optimization problem through the IP method [23]. Our obtained prototype filters are denoted HDPSS based filters (HDPSSb).

IV. OPTIMIZATION RESULTS

In order to make a fair comparison between QAM-FBMC and the proposed HQAM-FBMC, we optimized the HDPSSb prototype filter for different bandwidth values. As in [19], we have set $B = 1.7/M$, $B = 3/M$, and $B = 7/M$. Furthermore, the number of subcarriers was defined as $M = 128$, and the

$$A_g\left(\Delta_n'T, \Delta_k F\right) =$$
$$= \int_{-\infty}^{+\infty} g\left(t - n'T - \frac{\mathrm{mod}(k',2)}{2}T\right) g^*\left(t - nT - \frac{\mathrm{mod}(k,2)}{2}T\right) e^{-j2\pi F(k-k')(t + \frac{\mathrm{mod}(k,2)}{2} - n' - \frac{\mathrm{mod}(k',2)}{2})T}\,\mathrm{d}t$$
$$= \int_{-\infty}^{+\infty} g\left(t - n'T - \frac{\mathrm{mod}(k',2)}{2}T\right) g^*\left(t - nT - \frac{\mathrm{mod}(k,2)}{2}T\right) e^{-j2\pi F(k-k')t}\,\mathrm{d}t\ e^{-j2\pi(k-k')\left(\frac{\mathrm{mod}(k,2) - \mathrm{mod}(k',2)}{2} - n'\right)}$$

$$(10)$$

filter overlapping factor was chosen as $K = 4$. Thus, the proposed filters have length $L_g = KM = 512$. Besides, we established the threshold $\xi = 0.99$ for the eigenvalues, which means that we selected all eigenvectors corresponding to the eigenvalues greater than 0.99. By doing this more than 0.99 % of the power spectrum energy is within the considered bandwidth B. Although we have defined $\xi = 0.99$, this value can be defined according to the desired energy concentration. Furthermore, the eigenvector with the highest energy concentration is called the prolate window.

In Fig. 2, 3, and 4, we present the ambiguity function of the optimized HDPSSb filters. As we can notice, the interference spreads differently for each filter, and as expected, by increasing the optimized bandwidth we also increase the interference spreading in the frequency domain.
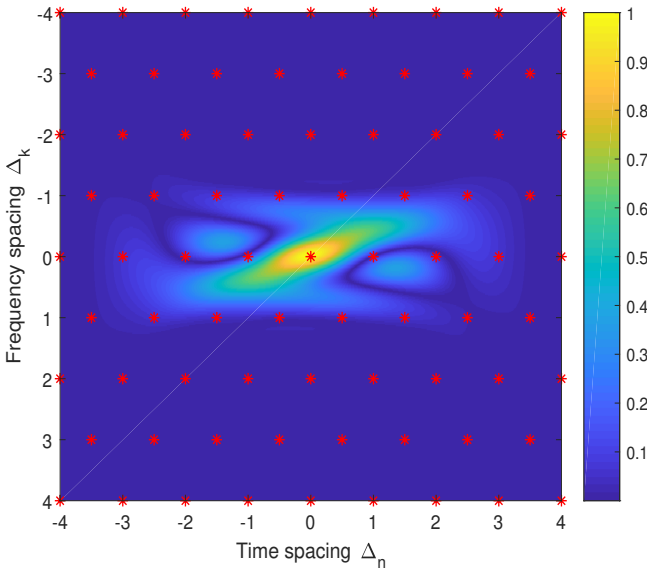

Fig. 3: Ambiguity function of the proposed HDPSSb filter $3/M$, $(|A_g(T, F)|)$.

Fig. 2: Ambiguity function of the proposed HDPSSb filter $1.7/M$, $(|A_g(T, F)|)$.

The red marks in Fig. 2, 3, and 4, represent the hexagonal lattice structure of the HQAM-FBMC system. These points, except for the central one $((\Delta_k, \Delta_n) = (0,0))$, indicate where we should sample the ambiguity function to obtain the coefficients that will be used to compute the intrinsic interference.

Furthermore, to make a comparison of the prototype filters, we present in Table I some characteristics of the DPSSb
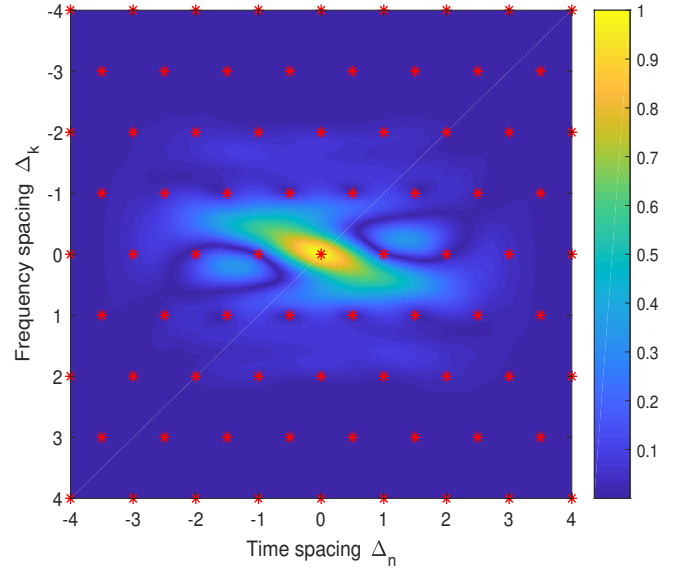

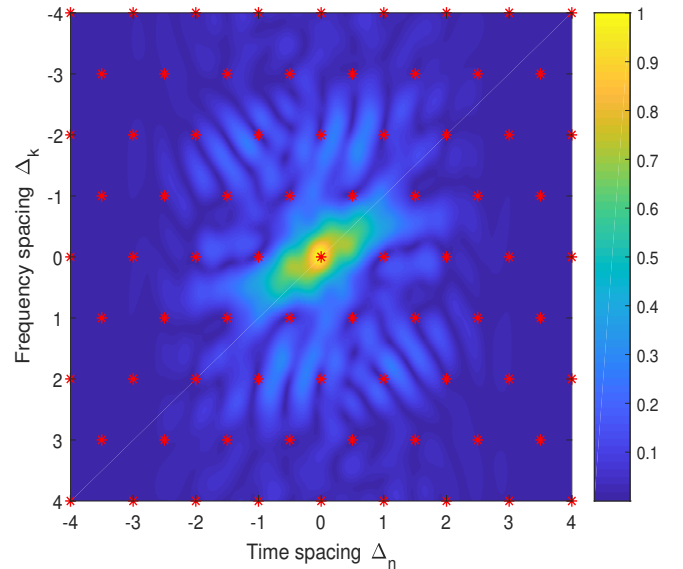
Fig. 4: Ambiguity function of the proposed HDPSSb filter $7/M$, $(|A_g(T, F)|)$.

filters [19] and the proposed HDPSSb filters. We also compare the inter-symbol interference (ISI) observed in a QAM-FBMC system when using DPSSb prototype filters, with the ISI observed in HQAM-FBMC system when using HDPSSb prototype filters. Finally we compare the out-of-band energy (OOBE) of each filter. It is also worth mentioning that all optimized filters have complex coeficients.

TABLE I: ISI and OOBE of different systems and filters.

Filter	ISI	OOBE
DPSSb 7/M	-18.95 dB	4.21e-06
HDPSSb (proposed) 7/M	-18.12 dB	2.70e-05
DPSSb 3/M	-14.47 dB	3.30e-05
HDPSSb (proposed) 3/M	-14.44 dB	3.55e-05
DPSSb 1.7/M	-12.60 dB	3.54e-04
HDPSSb (proposed) 1.7/M	-12.64 dB	3.43e-04

Similarly to what happen in the case of DPSSb filters, when optimizing HDPSSb filters, by increasing the desired transmission bandwidth it is possible to decrease the ISI of the optimized prototype filter. However, it happens at a cost of OOBE augmentation. We can also observe that the ISI level achieved is approximately the same for both filters DPSSb and HDPSSb with the same bandwidth.

V. PERFORMANCE EVALUATION

In this section, we evaluate and compare the system performance of QAM-FBMC using the DPSSb filter proposed in [19] with the system performance of HQAM-FBMC using our proposed and optimized prototype filters HDPSSb. For this, the size of the QAM-FBMC symbol was defined as $M = 128$, and we have simulated 500 symbols. Since the overlapping factor is $K = 1$, the filter has the same length as the FBMC symbol $L_g = 128$. We also considered different modulation levels, 4-QAM, 16QAM, and 64QAM. Performances were compared through the bit error rate (BER) of the systems over the AWGN channel and also over the pedestrian channel defined by 3GPP [24]. We have also performed the simulation considering 1000 Monte Carlo realizations.

In Fig. 5 and 6 we compare the performance of QAM-FBMC and HQAM-FBMC over AWGN channel. The modulation level in Fig. 5 was 4-QAM, and in Fig. 6 was 16-QAM. Both systems used optimized filters with bandwidth $B = 1.7/M$. As we can see, the results for QAM-FBMC and HQAM-FBMC are the same in both cases, 4-QAM and 16QAM, which means that the use of the hexagonal lattice did not bring any gain to the BER performance over the AWGN channel.

We have also used the intrinsic interference cancellation (IIC) technique in order to improve the overall system performance. And once again, for each IIC iteration both systems achieve the same results.

We have also evaluated and compared the system performance over pedestrian channel. The results were obtained by using several instantaneous channel realizations. In Fig. 7, 8, and 9, we compare the performance of QAM-FBMC and HQAM-FBMC. The modulation levels were 4-QAM, 16-QAM and 64-QAM respectively. We have also used the optimized filter with bandwidth $B = 1.7/M$.
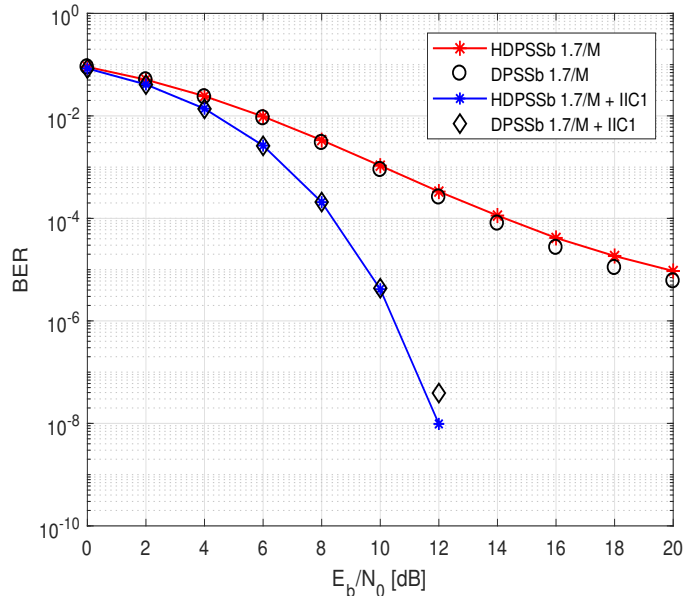

Fig. 5: BER performance of QAM-FBMC system with 4-QAM modulation with DPSSb $1.7/M$ filter and HQAM-FBMC with HDPSSb filter over AWGN channel.
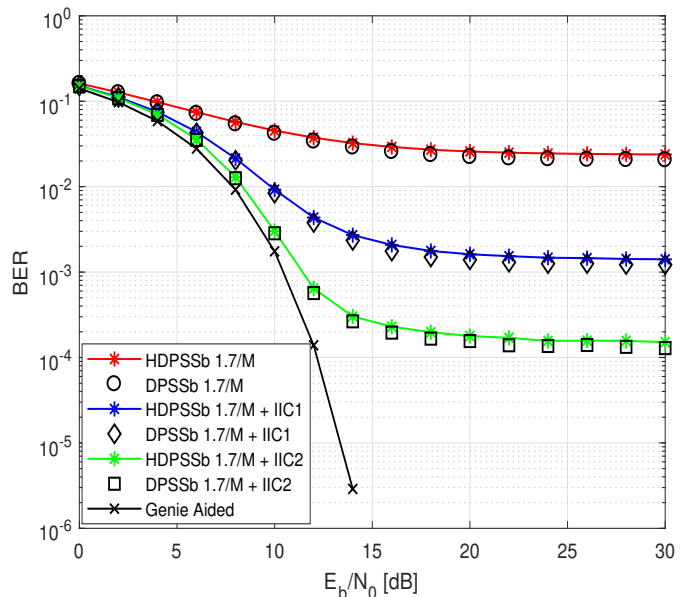

Fig. 6: BER performance of QAM-FBMC system with 16QAM modulation with DPSSb $1.7/M$ filter and HQAM-FBMC with HDPSSb $1.7/M$ filter over AWGN channel.

As shown in Fig. 7, for 4-QAM, we observe a performance gain of approximately 2 dB of HQAM-FBMC compared to QAM-FBMC. However, in the case of 16QAM, and 64QAM the results of HQAM-FBMC match perfectly with those of QAM-FBMC, even considering the IIC procedure. It is not possible to identify any gain in the BER performance when using an hexagonal lattice.

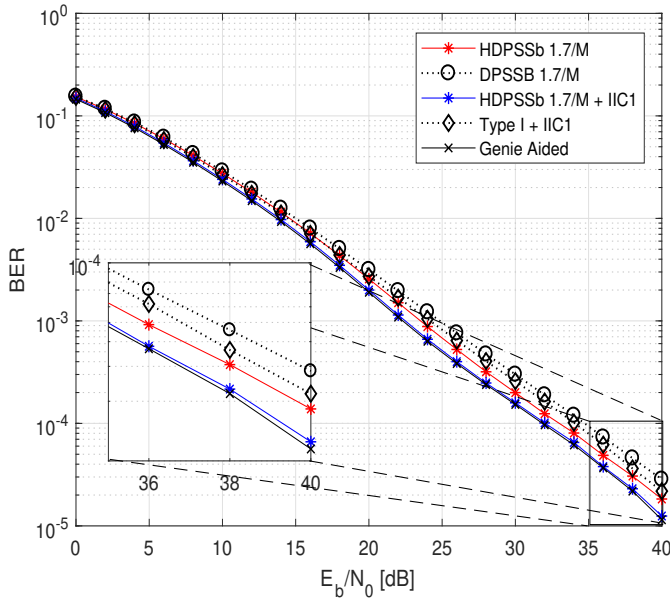The optimized filter with bandwidth $3/M$ was also eval-

Fig. 7: BER performance of QAM-FBMC system with 4-QAM modulation with DPSSb $1.7/M$ filter and HQAM-FBMC with HDPSSb $1.7/M$ filter over pedestrian channel.
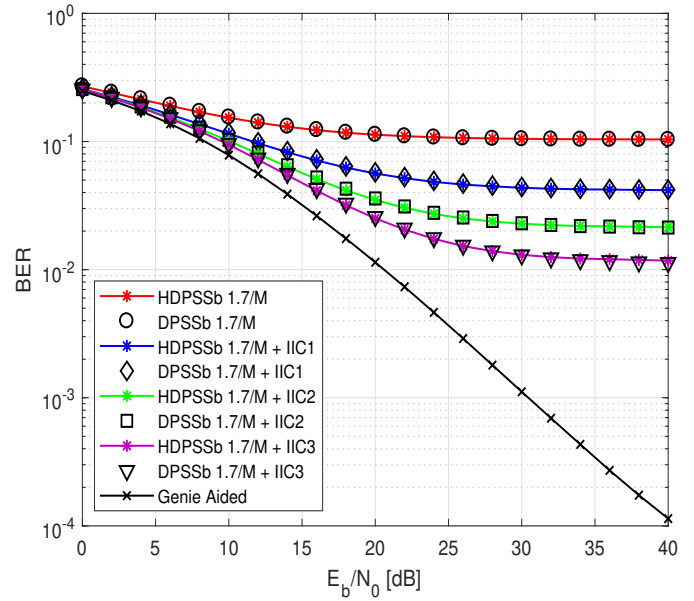

Fig. 9: BER performance of QAM-FBMC system with 64QAM modulation with DPSSb $1.7/M$ filter and HQAM-FBMC with HDPSSb $1.7/M$ filter over pedestrian channel.
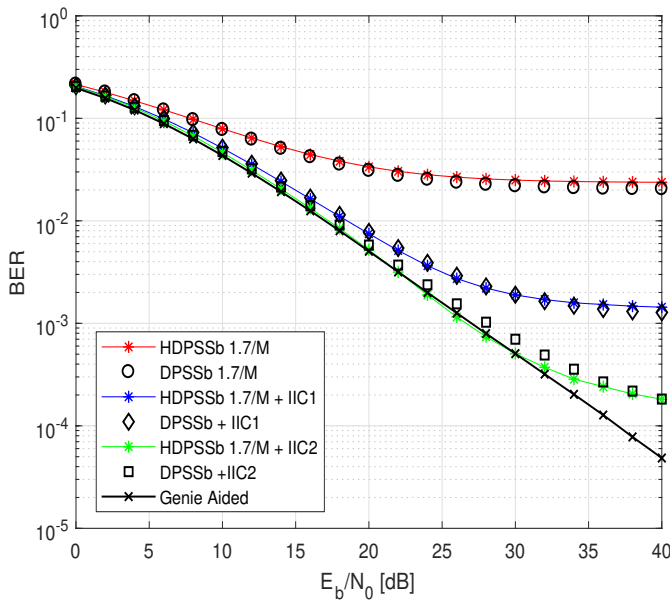

Fig. 8: BER performance of QAM-FBMC system with 16QAM modulation with DPSSb $1.7/M$ filter and HQAM-FBMC with HDPSSb $1.7/M$ filter over pedestrian channel.
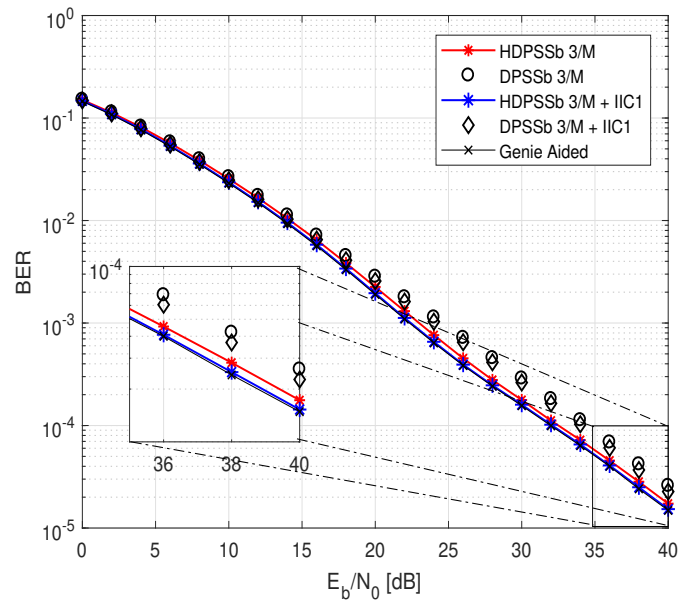

Fig. 10: BER performance of QAM-FBMC system with 4-QAM modulation with DPSSb $3/M$ filter and HQAM-FBMC with HDPSSb $3/M$ filter over pedestrian channel.

uated over pedestrian channel with 4-QAM, 16QAM, and 64QAM as presented in Fig. 10, 11, and 12, respectively.

Once again, as we can see in Fig. 10, the results of HQAM-FBMC with its optimized HDPSSb filter slightly outperform the one of QAM-FBMC using the optimized DPSSb filter in the case of 4-QAM modulation. Besides, for the case of 16-QAM and 64-QAM, presented in Fig. 11, and 12, respectively,

the evaluated performances are exactly the same. As shown in Fig. 11 when applying one iteration of the IIC procedure, we can observe a gain of 2dB at BER=10^{-3} for HQAM-FBMC with HDPSSb $3/M$ compared to QAM-FBMC.

The same conclusions can be drawn for the optimized filter with bandwidth $7/M$ with 4-QAM, 16QAM, and 64QAM as presented in Fig. 13, 14, and 15 respectively.

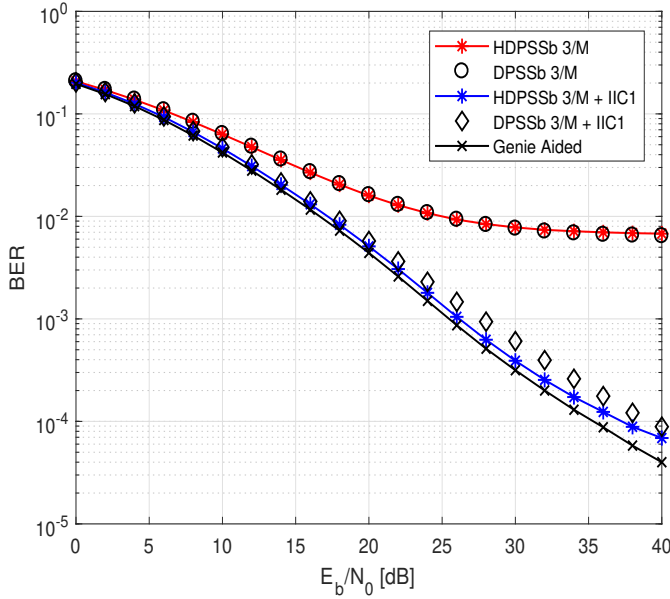For all test scenarios considering optimized filters, there was

Fig. 11: BER performance of QAM-FBMC system with 16QAM modulation with DPSSb $3/M$ filter and HQAM-FBMC with HDPSSb $3/M$ filter over pedestrian channel.

Fig. 13: BER performance of QAM-FBMC system with 4-QAM modulation with DPSSb $7/M$ filter and HQAM-FBMC with HDPSSb $7/M$ filter over pedestrian channel.

Fig. 12: BER performance of QAM-FBMC system with 64QAM modulation with DPSSb $3/M$ filter and HQAM-FBMC with HDPSSb $3/M$ filter over pedestrian channel.
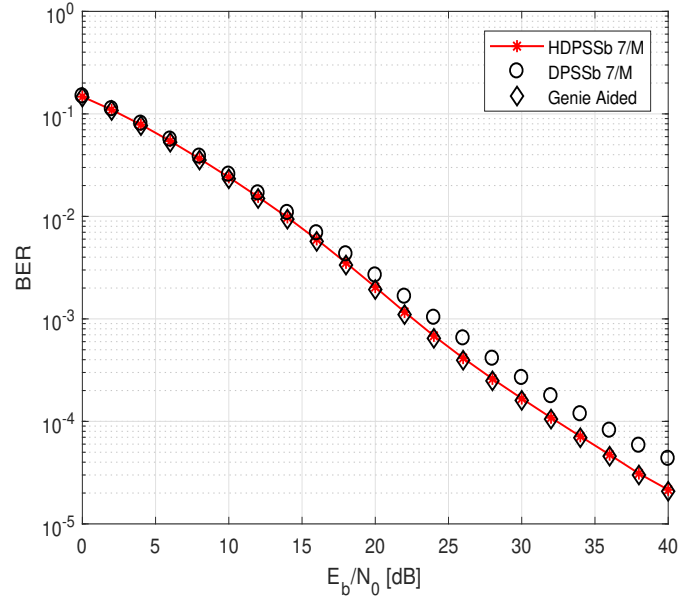

Fig. 14: BER performance of QAM-FBMC system with 16QAM modulation with DPSSb $7/M$ filter and HQAM-FBMC with HDPSSb $7/M$ filter over pedestrian channel.
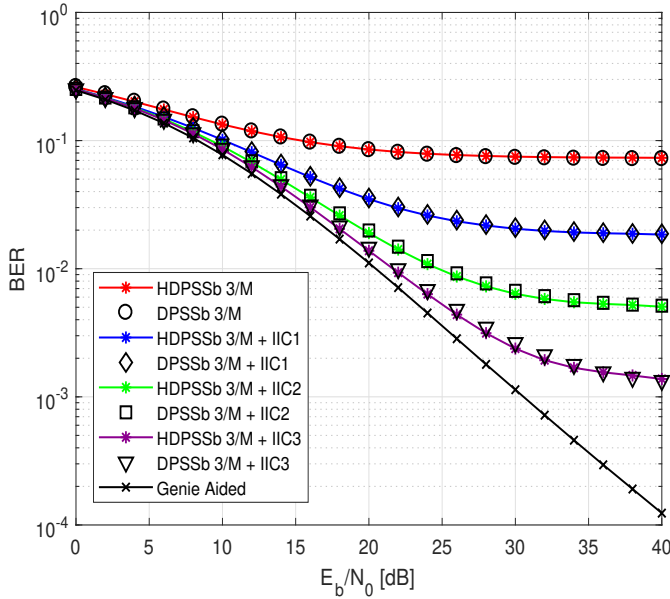
no gain in using the hexagonal lattice, except when considering 4-QAM modulation, where a performance gain of about 2dB for BER less than 10^{-3} can be obtained using HQAM-FBMC compared to QAM-FBMC.

VI. CONCLUSIONS

We proposed and analyze in this paper a novel structure of QAM-FBMC systems based on a hexagonal lattice. Unlike the

work found in the literature, where Gaussian filters are used, we applied a prototype filter specifically designed considering the hexagonal lattice. We proposed a prototype filter design based on DPSS, which leads to the filters named HDPSSb prototype filters. The proposed filters were also optimized to reduce intrinsic interference in HQAM-FBMC.

Moreover, we have also analyzed the gain of using an hexagonal lattice in QAM-FBMC systems.
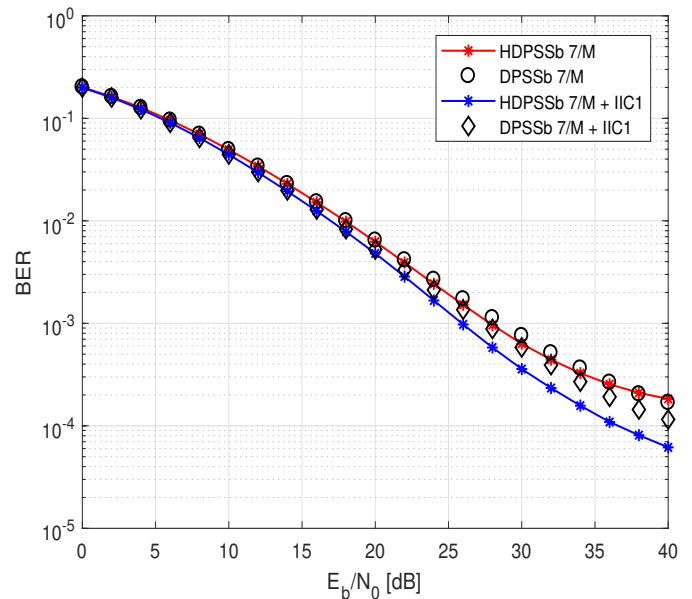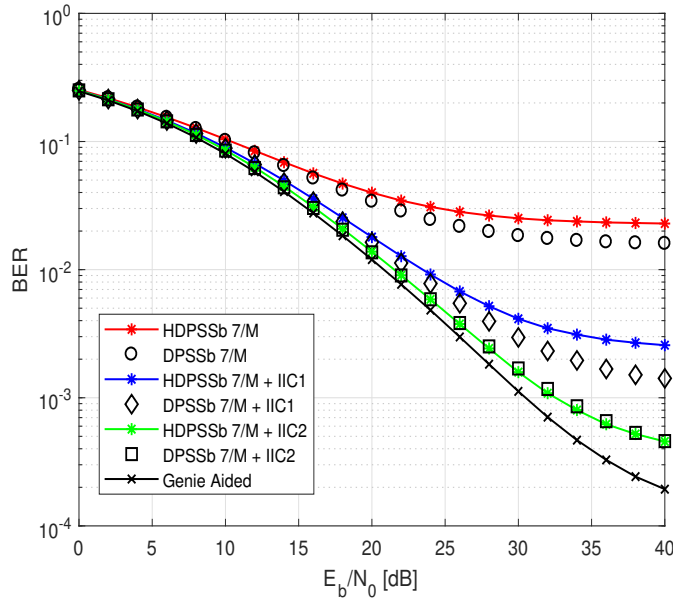
Fig. 15: BER performance of QAM-FBMC system with 64QAM modulation with DPSSb $7/M$ filter and HQAM-FBMC with HDPSSb $7/M$ filter over pedestrian channel.

The study conducted in this paper has demonstrated that the hexagonal lattice structure, when using optimized filters, is not appealing for QAM FBMC except for 4-QAM modulation, despite the literature advocating that it is beneficial in several applications.

REFERENCES

[1] Y. Medjahdi, S. Traverso, R. Gerzaguet, H. Shaiek, R. Zayani, D. Demmer, R. Zakaria, J.-B. Doré, M. B. Mabrouk, D. Le Ruyet *et al.*, "On the road to 5G: Comparative study of physical layer in MTC context," *IEEE Access*, vol. 5, pp. 26 556–26 581, 2017, DOI 10.1109/ACCESS.2017.2774002.

[2] T. Kebede, Y. Wondie, J. Steinbrunn, H. Belay, and K. Kornegay, "Multicarrier Waveforms and Multiple Access Strategies in Wireless Networks: Performance, Applications and Challenges," *IEEE Access*, 2022, DOI 10.1109/ACCESS.2022.3151360.

[3] M. Bellanger, D. Le Ruyet, D. Roviras, M. Terré, J. Nossek, L. Baltar, Q. Bai, D. Waldhauser, M. Renfors, T. Ihalainen *et al.*, "FBMC physical layer: a primer," *PHYDYAS, January*, vol. 25, no. 4, pp. 7–10, 2010.

[4] R. T. Kobayashi and T. Abrao, "Closed-form bit error probabilities for FBMC systems," *IEEE Trans. on Veh. Technol.*, vol. 69, no. 2, pp. 1237–1244, 2019.

[5] R. Zakaria and D. Le Ruyet, "Intrinsic interference reduction in a filter bank-based multicarrier using QAM modulation," *Elsevier - Phys. Commun.*, vol. 11, pp. 15–24, 2014, DOI 10.1016/j.phycom.2013.10.005.

[6] H. Nam *et al.*, "A New Filter-Bank Multicarrier System With Two Prototype Filters for QAM Symbols Transmission and Reception," *IEEE Trans. on Wireless Commun.*, vol. 15, no. 9, pp. 5998–6009, 2016, DOI 10.1109/TWC.2016.2575839.

[7] A. Sahin, I. Guvenc, and H. Arslan, "A survey on multicarrier communications: Prototype filters, lattice structures, and implementation aspects," *IEEE commun. Surveys & Tuts.*, vol. 16, no. 3, pp. 1312–1338, 2013, DOI 10.1109/SURV.2013.121213.00263.

[8] T. Strohmer and S. Beaver, "Optimal OFDM design for time-frequency dispersive channels," *IEEE Trans. on Commun.*, vol. 51, no. 7, pp. 1111–1122, 2003, DOI 10.1109/TCOMM.2003.814200.

[9] W. Kozek and A. F. Molisch, "Nonorthogonal pulseshapes for multicarrier communications in doubly dispersive channels," *IEEE J. Sel. Areas Commun.*, vol. 16, no. 8, pp. 1579–1589, 1998, DOI 10.1109/49.730463.

[10] B. Le Floch, M. Alard, and C. Berrou, "Coded orthogonal frequency division multiplex [tv broadcasting]," *Proc. IEEE Proc. IRE* (through 1962)*, vol. 83, no. 6, pp. 982–996, 1995.

[11] T. Strohmer, "Approximation of dual gabor frames, window decay, and wireless communications," *Applied and Computational Harmonic Analysis*, vol. 11, no. 2, pp. 243–262, 2001, DOI 10.1006/acha.2001.0357.

[12] H. Bölcskei, *Orthogonal Frequency Division Multiplexing Based on Offset QAM*. Boston, MA: Birkhäuser Boston, 2003, pp. 321–352, DOI 10.1007/978-1-4612-0133-5_12.

[13] J. H. Conway and N. J. A. Sloane, *Sphere packings, lattices and groups*. Springer-Verlag New York, 1993, DOI 10.1007/978-1-4757-2249-9.

[14] F.-M. Han and X.-D. Zhang, "Hexagonal multicarrier modulation: A robust transmission scheme for time-frequency dispersive channels," *IEEE Trans. on Signal Process.*, vol. 55, no. 5, pp. 1955–1961, 2007, DOI 10.1109/TSP.2006.890884.

[15] S. Peng, A. Liu, X. Pan, and H. Wang, "Hexagonal multicarrier faster-than-Nyquist signaling," *IEEE Access*, vol. 5, pp. 3332–3339, 2017, DOI 10.1109/ACCESS.2017.2674666.

[16] S. Peng, A. Liu, X. Tong, K. Wang, and G. Colavolpe, "Optimal multicarrier faster-than-Nyquist signaling under symbol-by-symbol detection," *Dig. Signal Process.*, vol. 72, pp. 135–146, 2018, DOI 10.1016/j.dsp.2017.10.014.

[17] H. Han, N. Kim, and H. Park, "Design of QAM-FBMC waveforms considering MMSE receiver," *IEEE Commun. Lett.*, vol. 24, no. 1, pp. 131–135, 2019, DOI 10.1109/LCOMM.2019.2952375.

[18] T. Jang, J. Kim, and J. H. Cho, "A Design of Spectrally-Efficient Low-Complexity QAM-FBMC Systems With Mismatched Prototype Filters," *IEEE Trans. on Veh. Technol.*, 2022, DOI 10.1109/TVT.2022.3200331.

[19] I. Galdino, R. Zakaria, D. Le Ruyet, and M. L. R. de Campos, "Prototype Filter for QAM-FBMC Systems Based on Discrete Prolate Spheroidal Sequences (DPSS)," *IEEE Access*, 2021, DOI 10.1109/ACCESS.2022.3157304.

[20] P. M. Woodward, *Probability and Information Theory, with Applications to Radar*. Pergamon London, 1953.

[21] D. Slepian, "Prolate spheroidal wave functions, Fourier analysis, and uncertainty—V: The discrete case," *Bell System Technical Journal*, vol. 57, no. 5, pp. 1371–1430, 1978, DOI 10.1002/j.1538-7305.1978.tb02104.x.

[22] T. Zemen and C. F. Mecklenbrauker, "Time-variant channel estimation using discrete prolate spheroidal sequences," *IEEE Trans. on Signal Processing*, vol. 53, no. 9, pp. 3597–3607, 2005, DOI 10.1109/TSP.2005.853104.

[23] S. Boyd and L. Vandenberghe, *Convex optimization*. Cambridge University press, 2004, DOI 10.1017/CBO9780511804441.

[24] "3GPP TS 36.104 - Base Station (BS) radio transmission and reception." [Online]. Available: https://portal.3gpp.org/desktopmodules/Specifications/SpecificationDetails.aspx?specificationId=2412

Iandra Galdino (ORCD 0000-0002-3564-2092) received the Engineering Degree in Telecommunications Engineering from the Fluminense Federal University (UFF), Niterói-RJ, Brazil, in 2015, the M.Sc. degree in Electrical Engineering from Federal University of Rio de Janeiro (COPPE/UFRJ) in 2017, and the Ph.D. degree in Electrical Enginering from the COPPE/UFRJ and also from CEDRIC/LAETITIA Research Laboratory, Conservatoire National des Arts et Métiers (CNAM), Paris, France.

She is currently post-doctor fellow with the MidiaCom Laboratory at the Institute of Computing of UFF, Niterói-RJ, Brazil.

Her areas of interest include communication systems, multicarrier waveforms and signal processing. Her current research includes waveform design for post 5G systems and signal processing applied to health monitoring techniques.

Rostom Zakaria (ORCD 0000-0002-4714-5763) received the engineering degree in electronics from the University of Science and Technology Houari Boumediene, Algiers, Algeria, in 2007, and the M.Sc. degree from the University of Paris-Est de Marne-La-Vallée, France, in 2008, and the Ph.D. degree from the CEDRIC/LAETITIA Research Laboratory, Conservatoire National des Arts et Métiers (CNAM), Paris, in 2012.

From 2012 until 2018, he has been temporary Assistant Professor and Researcher with CNAM. In 2016, he spent one month as Visiting Research Fellow at the Department of Electrical and Computer Engineering, Seoul National University (SNU), Seoul, South Korea. Since 2018, he is a Freelance Research Consultant and Lecturer where he worked for HUAWEI Paris Research Center during two years and provided 11 patent ideas on beyond 5G waveforms. He was one of the recipients of the Timely Incentive Team Award, and the President Award, Best Technology Innovation Award from the HUAWEI Paris research center in 2019 and 2020, respectively.

His main research interests are related in general to digital communications and signal processing including in particular interference cancellation techniques, filtered multicarrier modulations, and waveform design for next generation wireless communications.

Didier Le Ruyet (M'98, SM'11) (ORCD 0000-0002-9673-2075) received his Eng. Degree and his Ph. D. degree from Conservatoire National des Arts et Métiers (CNAM) in 1994 and 2001 respectively. In 2009, he received the "Habilitation à diriger des recherches" from Paris XIII University. From 1988 to 1996 he was a Senior Member of the Technical Staff at SAGEM Defence and Telecommunication, France. He joined Signal and Systems Laboratory, CNAM, Paris as a research assistant in 1996. From 2002 to 2010, he was an assistant professor at CNAM Paris. Since 2010 he is full professor at CNAM in the CEDRIC research laboratory. From 2016 until 2019 he was the deputy director of the CEDRIC.

He has published about 200 papers in refereed journals and conference proceedings and published five books in the area of digital communication.

He has been involved in several National and European projects dealing with multicarrier transmission techniques and multi-antenna transmission. He served as Technical Program Committee member in major IEEE ComSoc and VTS conferences, and as General Chair of the ninth edition of ISWCS'2012 conference and the Co-Chair of the ISWCS 2013 and 2019 edition.

His main research interests lie in the areas of digital communications and signal processing including channel coding, detection and estimation algorithms, filter-bank based multi-carrier communication and multi-antenna transmission.

Marcello L. R. de Campos (ORCD 0000-0002-6737-589X) was born in Niterói, Brazil, in 1968. He received the Engineering degree (cum laude) from the Federal University of Rio de Janeiro (UFRJ), Rio de Janeiro, Brazil, in 1990, the M.Sc. degree from COPPE/UFRJ in 1991, and the Ph.D. degree from the University of Victoria, Victoria, BC, Canada, in 1995, all in Electrical Engineering.

In 1996, he was post-doctoral fellow with the Department of Electronics, School of Engineering, UFRJ, and with the Program of Electrical Engineering, COPPE/UFRJ. From January 1997 until May 1998, he was Associate Professor with the Department of Electrical Engineering (DE/3), Military Institute of Engineering (IME), Rio de Janeiro. He is currently Deputy Director for Academic Affairs at COPPE/UFRJ and Professor of the Program of Electrical Engineering, where he has also served as Department Vice-Chair and Chair in the years 2004 and 2005, respectively. As visiting scholar, he has spent small sabbatical periods at the Laboratory for Telecommunications Technology, Helsinki University of Technology, Espoo, Finland, at the Centre for Wireless Communications, University of Oulu, Oulu, Finland, at the University Graduate Center of the University of Oslo, Oslo, Norway, at Aalto University, Helsinki, Finland, and at the Norwegian University of Science and Technology, Trondheim, Norway.

Prof. Campos served as IEEE Communications Society Regional Director for Latin America in 2000 and 2001, Local-Arrangements Co-Chair for GLOBECOM'99, Finance Chair for SPAWC 2008, Plenary Chair for ISCAS 2011, and Technical Co-Chair for the 2013 Brazilian Telecommunications Symposium. He founded and was the Chair of the IEEE Signal Processing Society Rio de Janeiro Chapter for four years. He has taught over 150 courses on mobile communications in 15 countries, and managed numerous R&D projects in signal processing and communications for technology companies in Brazil and abroad. His research interests include adaptive signal processing in general and its application to distributed networks in particular, adaptive beamforming, statistical signal processing, statistical and machine learning, optimization, signal processing for communications, underwater, mobile and wireless communications, and MIMO systems. He is a CNPq productivity researcher level 1-D, his curriculum vitae can be retrieved from http://lattes.cnpq.br/2402401592333107, and he is associated with the Signals, Multimedia, and Signal Processing Laboratory (www.smt.ufrj.br) at COPPE/UFRJ.